Earthline Journal of Chemical Sciences
E-ISSN: 2581-9003; CODEN: EJCSB4
Volume 9, Number 1, 2023, Pages 17-45
https://doi.org/10.34198/ejcs.9123.1745

Experimental and Theoretical Assessments on Anticorrosion Performance of 2-(1H-benzimidazol-2-yl)-3-(4-hydroxyphenyl) Acrylonitrile for Copper in 1M HNO_3

Mougo André Tigori[1,*], Aboudramane Koné[1], Koffi Amenan Mireille[1], Drissa Sissouma[2] and Paulin Marius Niamien[2]

[1] Laboratoire des Sciences et Technologies de l'Environnement, UFR Environnement, Université Jean Lorougnon Guédé, BP 150 Daloa, Côte d'Ivoire

[2] Laboratoire de Constitution et de Réaction de la Matière, UFR SSMT, Université Félix Houphouët-Boigny, 22 BP 582 Abidjan 22, Côte d'Ivoire

[*] Corresponding author's email: tigori20@yahoo.fr

Abstract

The present study was designed to determine the inhibition effect of 2-(1H-benzimidazol-2-yl)-3-(4-hydroxyphenyl) acrylonitrile in 1M HNO_3 using a combined experimental and theoretical approach. Mass loss techniques revealed that 2-(1H-benzimidazol-2-yl)-3-(4-hydroxyphenyl) acrylonitrile inhibition efficiency is dependent on its concentration and temperature. It has been shown that the studied molecule inhibits copper corrosion by an adsorption behavior by donating and accepting electrons. Kinetic parameters have been determined and discussed. Quantum chemical parameters calculated by means of density functional theory (DFT) have shown that studied molecule reactivity is strongly related to the electronic properties, which could help to understand the molecule-metal interactions. The reactive sites have been determined by means of Fukui Functions and dual descriptor. Quantitative structure-property relationship (QSPR) model introduced in this study was used to find a set of quantum chemical parameters capable of correlating the experimental and theoretical data in order to design more suitable organic corrosion inhibitors. The theoretically obtained results were found to be consistent with the experimental data reported.

Received: August 24, 2022; Accepted: September 18, 2022; Published: September 25, 2022

Keywords and phrases: 2-(1H-benzimidazol-2-yl)-3-(4-hydroxyphenyl) acrylonitrile; mass loss; copper corrosion; DFT; QSPR.

1. Introduction

Because of its consequences on industrial equipment the corrosion of materials [1] is of great concern for various industries. It is in this context that copper metal structures corrosion is a phenomenon that has attracted the attention of researchers in recent years [2,3]. In fact, the strength of copper wire and the reliability of the contacts it provides are main reasons for its widespread use in the electrical industry, from construction to distribution, including the manufacture of electrical equipment and electronic components. Moreover, copper and its alloys are not attacked by water or by a large number of chemical products [4]. Often, during its use, these metallic copper structures are covered with scale. However, acidic solutions are widely used in various industries for cleaning copper in order to remove these scales [5]. These acid solutions promote the metal structures dissolution that have undergone this cleaning. In order to reduce this dissolution and to ensure the safety of users, manufacturers have resorted to the use of corrosion inhibitors [6-8]. According to them, the reliability, performance and safety of a large number of technical systems depend on the protection against corrosion. As a result the life service of metal equipment used in industry also depends on the type of protection. Inhibitors are substances that protect metals from corrosion by decreasing the rate of dissolution. Many compounds have been used as copper corrosion inhibitors [9-12]. Among these compounds, a distinction is made between organic and inorganic compounds. Unfortunately, most of these inorganic compounds and some organic molecules have been shown to be toxic and environmentally unfriendly, therefore, their use is limited due to environmental concerns [13,14]. So, the new organic inhibitors use that are less toxic, biodegradable and meet environmental standards are recommended [15-19]. Organic corrosion inhibitors containing nitrogen, sulfur, oxygen atoms and π-electrons in conjugated triple or double bonds are of increasing interest in the field of corrosion control. In addition, the stability of adsorbed inhibitor films formed on the metal surface to protect it from corrosion depends on these atoms and π-electrons [20-22].

The choice of 2-(1H-benzimidazol-2-yl)-3-(4-hydroxyphenyl) acrylonitrile as a copper corrosion inhibitor in this study is based on the existence in this molecule of some heteroatoms and (π)-bonds capable of providing electron transfer to metal surface. This molecule is an antifungal so it would not present a toxicity risk. The drugs use as corrosion inhibitors for metals in different aggressive environments is plebiscite nowadays with the aim of preserving the environment [23,24].

Experimental investigations can be interpreted by quantum chemical calculations [25,26]. These calculations can predict the inhibitory activity of organic compounds. Thanks to the progress in the technology of implementations have reached a point where predicted properties with reasonable accuracy can be obtained from the density function theory (DFT) [27-30]. The theoretical aspect based on density function theory and quantitative structure-property relationship have been addressed in this work to clearly explain the inhibition mechanism of studied molecule and to evaluate it structural properties and its inhibition ability.

Thus, the present study aims to investigate experimentally the inhibition effect of 2(1H-benzimidazol-2-yl)-3-(4-hydroxyphenyl) acrylonitrile of copper corrosion in 1M nitric acid solution and to correlate its inhibition efficiency with its molecular structure by using density function theory and quantitative structure-property and quantitative structure-property calculations. Finally, the expected results will allow a better understanding of electronic exchanges between inhibitor and copper, which results will be discussed with the studies reported in literature.

2. Experimental Procedure

2.1. Inhibitor and solutions

The benzimidazolyl acrylonitriles derivative used in the study, namely 2-(1H-benzimidazol-2-yl)-3-(4-hydroxyphenyl) acrylonitrile with an antifungal effect was synthesized in the Laboratory according to Van Allan method [31]. The molecular structure was identified by RMN-1H, 13C, spectroscopies and mass spectroscopy is given in Figure 1.

RMN 1H (DMSO-d6, δ ppm): 8.40 (1H, s, C=CH). 13C: 145.14 (C=CH); 116.04 (C≡N); 102.38 (C=CH). SM [EI, 70 eV]: 245 ([M]$^+$, 39); 244 ([M-H]$^+$, 96). Washing in hexane: 52%. PF: 222°C.

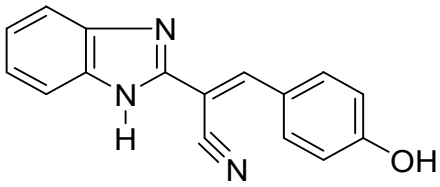

Figure 1. Molecular structure of 2-(1H-benzimidazol-2-yl)-3-(4-hydroxyphenyl) acrylonitrile (BHPA).

An aqueous aggressive solution of 1 M HNO_3 was prepared by dilution of analytical grade 65% HNO_3 from FISHER with double-distilled water. This solution was used as a blank solution in this experimental part. The different inhibitor concentrations that were prepared from this blank solution for the gravimetric tests were 10^{-3}mM, 5.10^{-3}mM, 10^{-2}mM and 3.10^{-2}mM.

2.2. Copper specimens preparation

Copper specimens in the form of a rod measuring 10 mm long and 2.2 mm in diameter were cut from commercial copper of 99.5% purity. Then these copper specimens were successively polished with metallographic emery papers of fineness varying from 150 to 600 grains. Finally, they were washed thoroughly with bidistilled water, degreased and dried with acetone, then rinsed again with bidistilled water and dried in a MEMMERT oven at 80°C for 20 minutes. This treatment aims to remove all traces of grease and native oxide before use.

2.3. Mass loss technique

The mass loss technique is the basic measurement method to evaluate corrosion because of its reliability in results. This method consists in determining the mass loss of a copper specimens (m_1) immersed in 1M HNO_3 solution for 1h in the absence and presence of namely 2-(1H-benzimidazol-2-yl)-3-(4-hydroxyphenyl) acrylonitrile. A water thermostat from RAYPA set at ±0.5°C maintains the temperature, ranging from 298K to 323K. After 1 hour elapsed time, each specimen was removed from the solution, rinsed thoroughly with bidistilled water, dried, and then reweighed (m_2) accurately.

2.4. Density function theory calculations

Quantum chemistry provides tools to interpret multiple chemical concepts used in different branches of chemistry. Indeed in this method, quantum chemical calculations using density functional theory (DFT) are performed to explore the relationship between the molecular properties of the inhibitor and the inhibition efficiency. In this study, all calculations were performed using Gaussian 09 Program [32] in the gas phase with the three-parameter Becke B3LYP hybrid Lee-Yang-Parr functional [33] in the base set 6-311G(d,p). In addition, these sets were chosen because they give very accurate results. A full optimization was performed using Gaussview 09 program package. The following quantum chemical quantities were computed: highest occupied molecular orbital energy (E_{HOMO}), lowest unoccupied molecular orbital energy (E_{LUMO}), energy gap (ΔE), dipole moment (μ), electron affinity (A), the ionization energy (I), electronegativity (χ),

hardness (η), softness (σ), electrophylicity index (ω), fraction of electron transferred (ΔN) and total energy (E_T). The reactivity sites analysis within the molecule was performed by the local quantities such as Fukui functions and dual descriptor.

2.5. Quantitative structure-property relationship calculations

This model was used to find a mathematical combination between experimental inhibition efficiency and the theoretical molecular parameters. These mathematical relations fitted to experimental values are intended to provide reliable theoretical tools capable of studying the interaction between the inhibitor with the metal surface in the acidic solution in order to estimate the inhibition efficiencies of molecules analogous to the molecule studied. In this approach experimental results were adapted to the empirical nonlinear model first proposed by Lukovits *et al.* [34] and verified by Khaled [35].This model is based on Langmuir adsorption isotherm and can be determined as follows:

$$IE_{calc}(\%) = \frac{[Ax_j + B]C_i}{1 + [Ax_j + B]C_i} * 100. \quad (1)$$

In this model the equations used to predict the theoretical inhibition efficiencies are determined from the inhibitor concentrations (C_i). A and B are real constants that will be determined when solving the system of equations.

3. Results and Discussion

3.1. Corrosion inhibition study

Corrosion rate (W), surface coverage (θ) and the inhibition efficiency (IE %) acquired by mass loss technique were determined by the following expressions:

$$W = \frac{\Delta m}{S_e.t} = \frac{m_1 - m_2}{S_e.t} \quad (2)$$

$$\theta = \frac{W_0 - W}{W_0} \quad (3)$$

$$IE(\%) = \frac{W_0 - W}{W_0} * 100 \quad (4)$$

Δm: is the mass loss (g), m_1 and m_2 are, respectively, the mass (g) before and after immersion in the solution test; t: the immersion time (h) ; S_e: the total surface of sample (cm^2) ; W_0 and W; are, respectively, the copper corrosion rates in the absence and presence of BHPA.

The evolution of inhibition efficiency versus concentration in BHPA for different temperature is presented in Figure 2.

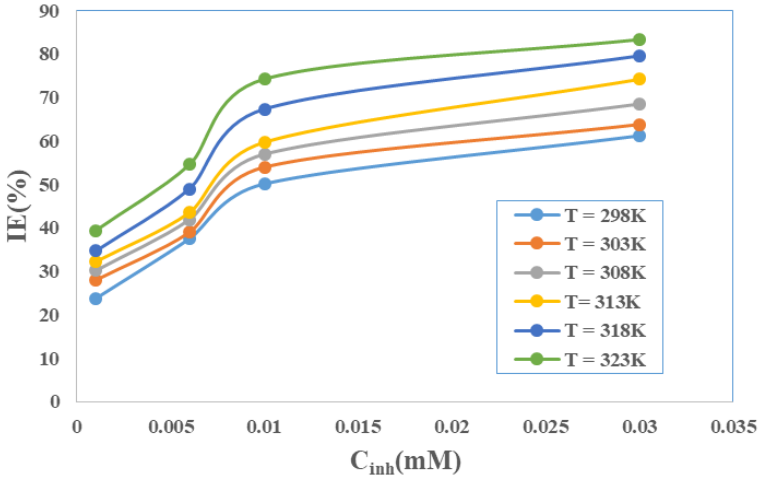

Figure 2. Inhibition efficiency of BHPA for different concentrations and temperatures.

Figure 3 indicates the Inhibition efficiency versus temperature for different concentrations.

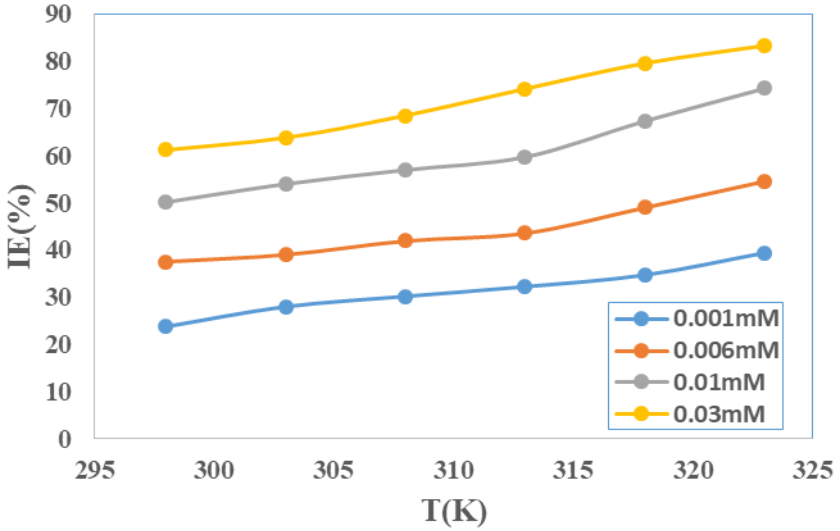

Figure 3. Inhibition efficiency versus temperature for different concentration of BHPA.

Figures 2 and 3 analysis indicate clearly that, BHPA inhibition efficiency increases with increasing temperature and inhibitor concentration. Thus temperature and inhibitor concentration combined action influences BHPA behavior on copper surface. It appears from these observations that BHPA adsorbs strongly on copper surface when temperature and concentration of BHPA increase. This adsorption favors the establishment of a protective layer which becomes thicker when the temperature and BHPA concentration increase. Accordingly, it is deduced that BHPA can effectively inhibit copper corrosion in 1 M.HNO_3 at high temperature.

3.2. Adsorption isotherm and thermodynamic adsorption parameters

Copper corrosion inhibition by BHPA in 1M HNO_3 results from its adsorption on metal surface. Indeed this process can be considered to a chemical reaction during which water molecules adsorbed on metal surface are replaced by the organic molecules coming within the solution. This reaction process between organic molecule within the solution $(Org_{(sol)})$ and the adsorbed water molecule $(H_2O_{(ads)})$ can be represented by the following reversible equation:

$$Org_{(sol)} + xH_2O_{(ads)} \rightleftarrows Org_{(ads)} + xH_2O_{(sol)} \quad (5)$$

In order to gain more insight into adsorption behaviour of the studied compounds, attempts were made to fit the experimental data into various adsorption isotherms including: Langmuir, Temkin, El-Awady and Freundlich. It is found from this study that Langmuir isotherm with the best fits obtained $(R^2 > 0.98)$ can better indicate the interaction between BHPA and copper surface. The equation of this isotherm is the following [36]:

$$\frac{C_{inh}}{\theta} = \frac{1}{K_{ads}} + C_{inh} \quad (6)$$

where C_{inh}: inhibitor concentration and K_{ads} adsorption equilibrium constant.

Figure 4 depicts the plots of $\frac{C_{inh}}{\theta}$ versus C_{inh}.

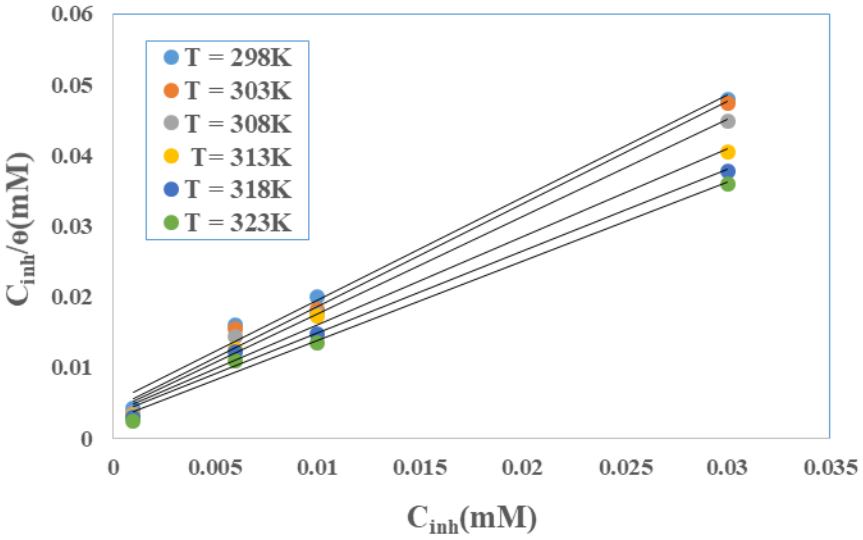

Figure 4. Langmuir adsorption isotherm plots for BHPA at different temperatures.

The straight lines obtained have slopes that are greater than unity for all temperatures. However, these deviations are attributed to interactions between the adsorbed species. Therefore Langmuir adsorption isotherm cannot be applied rigorously. Then this adsorption can be correctly described by the modified Langmuir model or isotherm of Villamil *et al.* [37]. The equation of this suitable model is given by:

$$\frac{C_{inh}}{\theta} = \frac{n}{K_{ads}} + nC_{inh} \tag{7}$$

where n is the slope of the plot and $n\theta$ is the effective covered surface fraction of the metal.

The suitable isotherm study leads to the determination of thermodynamic adsorption parameters adsorptions which are essential in metal corrosion inhibition study in a corrosive medium.

Thus the variation of adsorption free enthalpy (ΔG^0_{ads}) is expressed by the following relation:

$$\Delta G^0_{ads} = -RTln(55.5\ K_{ads}) \tag{8}$$

In this relation R is the gas constant, T is the absolute temperature, and 55.5 is the concentration of water (in mol/L) in the solution.

The values of K_{ads} (Adsorption Equilibrium Constant) are obtained from Villamil isotherm parameters.

Variation of adsorption enthalpy (ΔH^0_{ads}) and entropy (ΔS^0_{ads}) were deduced from the equation below:

$$\Delta G^0_{ads} = \Delta H^0_{ads} - T\Delta S^0_{ads} \quad (9)$$

The plot of ΔG^0_{ads} versus temperature (Figure 5) leads to these parameters: ΔS^0_{ads} and ΔH^0_{ads} were determined respectively from the intercept and the slope of the straight lines.

Villamil isotherm parameters and thermodynamic adsorption parameters are collected in Table 1.

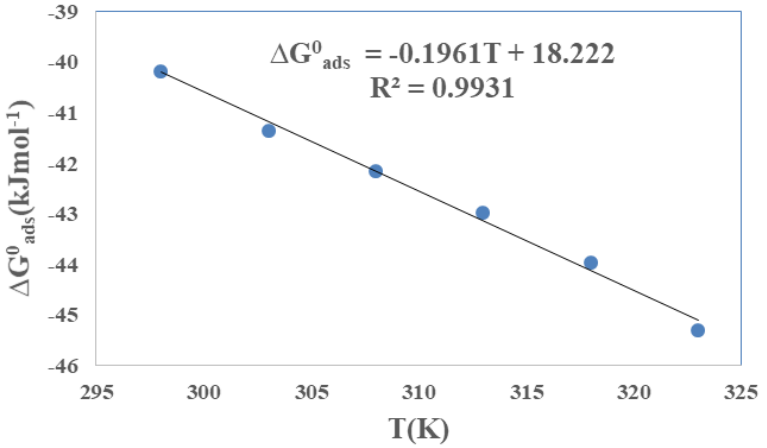

Figure 5. Variation of adsorption free enthalpy versus temperature.

Table 1. Villamil isotherm and thermodynamic adsorption parameters.

T (K)	Equation	R^2	K_{ads} $(10^3 M^{-1})$	ΔG^0_{ads} $(kJmol^{-1})$	ΔH^0_{ads} $(kJmol^{-1})$	ΔS^0_{ads} $(Jmol^{-1}K^{-1})$
298	$\frac{C_{inh}}{\theta} = 1.4482C_{inh} + 0.005$	0.9893	200.0	-40.17	18.22	196.1
303	$\frac{C_{inh}}{\theta} = 1.4526C_{inh} + 0.0041$	0.9895	243.9	-41.35		
308	$\frac{C_{inh}}{\theta} = 1.3759C_{inh} + 0.0039$	0.9915	256.4	-42.16		
313	$\frac{C_{inh}}{\theta} = 1.2419C_{inh} + 0.0037$	0.9847	270.3	-42.98		
318	$\frac{C_{inh}}{\theta} = 1.1557C_{inh} + 0.0033$	0.9897	303.0	-43.97		
323	$\frac{C_{inh}}{\theta} = 1.1207C_{inh} + 0.0026$	0.9928	384.6	-45.30		

The negative values of the variation of adsorption free enthalpy indicate that adsorption process is spontaneous while the adsorbed layer is stable [38]. ΔG^0_{ads} values obtained in this study are lower than -40 kJ/mol, thus reflecting chemisorption existence. In fact chemisorption is attributed to coordination bonds between N, O atoms of BHPA molecule and copper surface. According to previous studies if ΔG^0_{ads} values exceeds -20 kJ/mol physical adsorption exists while less than -40 kJ/mol concern chemical adsorption. Both adsorption modes exist in the range of -20 kJ/mol to -40 kJ/mol [39,40]). The increase in K_{ads}values with temperature reveals that increasing temperature enhance BHPA inhibition performance [41]. Therefore these results confirm the inhibition efficiencies obtained with the mass loss technique. Variation of adsorption enthalpy (ΔH^0_{ads}) values are positive indicating an exothermic process of BHPA adsorption on copper [41]. The increase in disorder created by water molecules desorption during BHPA molecules adsorption on copper is justified by the positive values of adsorption entropy variation [42] (ΔS^0_{ads}).

The study of adsorption parameters revealed that BHPA adsorbs on copper chemically. In order to definitively check this adsorption nature Adejo-Ekwenchi isotherm was used [43]. The equation of this isotherm is the following:

$$log\left(\frac{1}{1-\theta}\right) = logK_{AE} + blogC_{inh} \tag{10}$$

where K_{AE} and b are Adejo-Ekwenchi isotherm parameters. The plot of $log\left(\frac{1}{1-\theta}\right)$ versus $logC_{inh}$ is given by Figure 6.

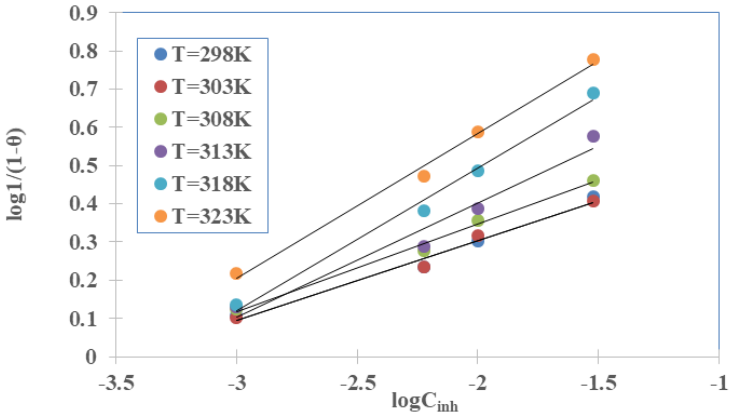

Figure 6. Adejo-Ekwenchi adsorption isotherm plots for BHPA at different temperatures.

The corresponding parameters to this isotherm deduced from the lines obtained are reported in Table 2.

Table 2. Adejo-Ekwenchi adsorption isotherm parameters.

T(K)	R^2	b	$logK_{AE}$	K_{AE}
298	0.9820	0.2083	0.2083	1.615
303	0.9848	0.2086	0.2086	1.616
308	0.9906	0.2298	0.2298	1.697
313	0.9597	0.2990	0.2990	1.990
318	0.991	0.3732	0.3732	2.361
323	0.9932	0.3796	0.3796	2.396

Analyzing Table 2, it can be seen that the parameters b and K_{AE} increase with increasing temperature, confirming the chemisorption preponderance [43].

3.3. Kinetic thermodynamic parameters

In an acidic environment, metal dissolution is generally influenced by temperature. The temperature accelerates the corrosion reactions. Indeed, the corrosion rate increases exponentially with the increase of temperature according to the following Arrhenius equation:

$$logW = logA - \frac{E_a}{2.3.R.T} \tag{11}$$

where W is the corrosion rate, E_a is the apparent activation energy, R is the universal gas constant, T is the absolute temperature and A is the frequency factor.

The transition state equation has been used for accessing the values of variations of enthalpy and entropy. It is expressed by following relation:

$$log\left(\frac{W}{T}\right) = log\left(\frac{R}{\aleph.h}\right) + \frac{\Delta S_a^*}{2.3.R} - \frac{\Delta H_a^*}{2.3.R.T} \tag{12}$$

In this relation: ΔS_a^* is variation of activation entropy, ΔH_a^* is variation of activation enthalpy, R is the perfect gas constant, $\aleph$ is Avogadro number and h is Planck's constant

To determine the apparent activation energy the plot of $logW$ versus $\frac{1}{T}$ (Figure 7) was used. The slopes of the straight lines obtained $\left(-\frac{E_a}{2.3.R}\right)$ permit to access to apparent activation energy values.

Figure 8 shows the plot of $log\left(\frac{W}{T}\right)$ versus $\frac{1}{T}$ which leads ΔS_a^* and ΔH_a^* values. In this case the slopes $\left(-\frac{\Delta H_a^*}{2.3.R}\right)$ and the intercepts $\left(log\left(\frac{R}{N.h}\right)+\frac{\Delta S_a^*}{2.3.R}\right)$ allowed to determine respectively ΔH_a^* and the ΔS_a^* values.

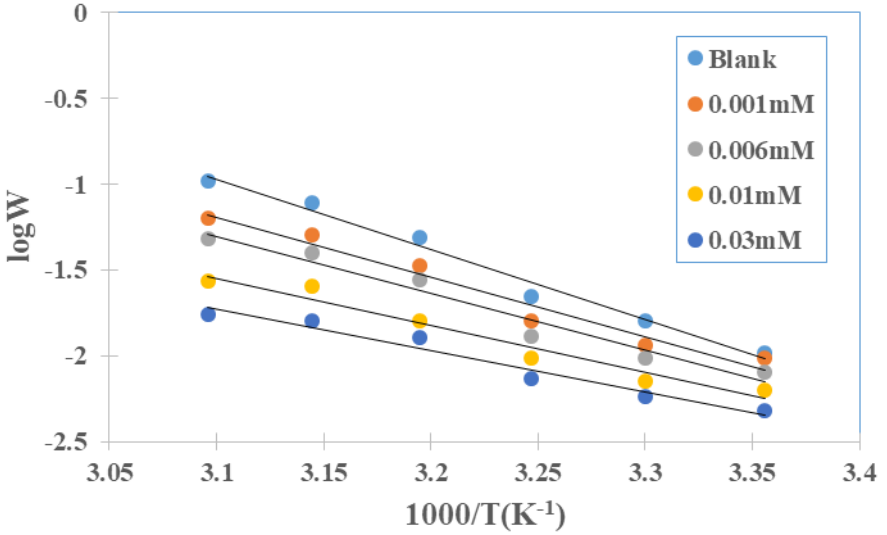

Figure 7. $LogW$ versus $\frac{1}{T}$ for different concentrations.

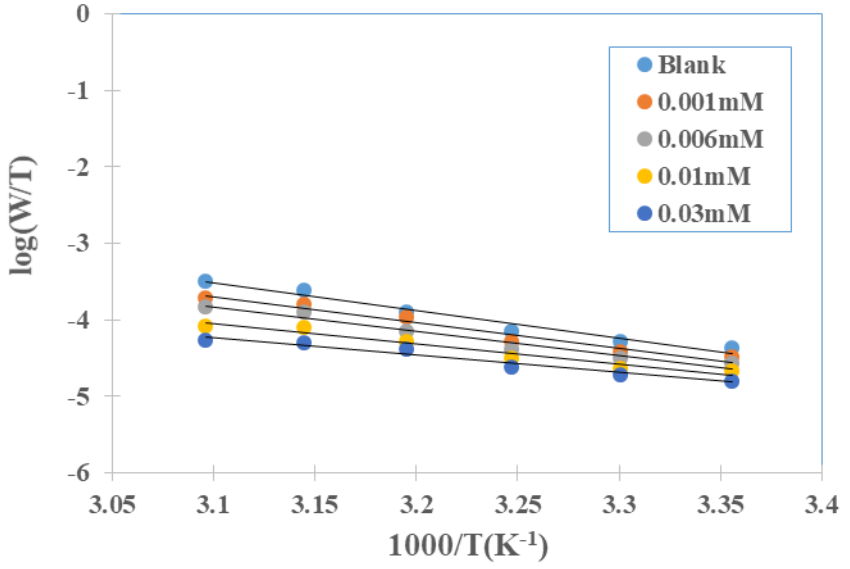

Figure 8. $Log\left(\frac{W}{T}\right)$ versus $\frac{1}{T}$ for different concentrations.

The copper dissolution parameters are recorded in Table 3.

Table 3. Dissolution parameters for copper in 1M HNO_3.

C_{inh} (mM)	$E_a(kJmol^{-1})$	$\Delta H_a^*(kJmol^{-1})$	$\Delta S_a^*(Jmol^{-1}K^{-1})$
0	78.4	69.43	-49.51
0.001	66.7	64.17	-69.32
0.006	63.8	60.06	-84.67
0.010	52.0	50.38	-118.83
0.030	46.2	43.59	-143.40

Table 3 inspection indicates that the apparent activation energy in BHPA presence are lower than the value obtained in its absence. However the activation mechanism is influenced by chemisorption [44]. This gradual decrease in activation energy in BHPA presence shows that initially copper dissolution is rapid. This dissolution is then attenuated by the formation of the Cu-Inh complex on copper surface.

The positive values of activation enthalpy variation (ΔH_a^*) indicate that copper dissolution reaction is endothermic [44]. The negative values of variation of activation entropy (ΔS_a^*) implies that the activated complex is an association [45,46]. It is also observed that the disorder decreases when the inhibitor concentration increases. A protective layer is then formed on copper surface as the temperature increases, justifying the increase in inhibition efficiency at high temperature.

3.4. Theoretical analysis

3.4.1. Inhibitor molecular reactivity

To prove the molecule reactivity and its ability to be a good inhibitor against corrosion, the global reactivity parameters of neutral (BHPA) molecule and its protonated form ($BHPAH^+$) were calculated. These parameters determined using DFT at 6-311G(d,p) level could allow to correlate the inhibition efficiencies obtained experimentally and to explain BHPA adsorption mechanism on copper surface. Optimized molecular structures of the neutral and protonated form of BHPA using DFT at 6-311G(d,p) are displayed by Figure 9. They are listed in Table 4.

Table 4. Calculated global reactivity parameters obtained by DFT/6-311G(d,p).

Parameters	BHPA	$BHPAH^+$
E_{HOMO} (eV)	-5.8491	-8.7084
E_{LUMO} (eV)	-2.4347	-5.7088
ΔE (eV)	3.4147	2.9393
μ (Debye)	3.2447	21.2608
$I = -E_{HOMO}$ (eV)	5.8491	8.7084
$A = -E_{LUMO}$ (eV)	2.4347	5.7088
$\chi = -\mu_p = \frac{I+A}{2}$ (eV)	4.1419	7.2086
$\eta = \frac{I-A}{2}$ (eV)	1.7073	1.4697
$\sigma = \frac{1}{\eta}$ $(eV)^{-1}$	0.5857	0.6804
$\Delta N = \frac{\chi_{cu} - \chi_{inh}}{2(\eta_{cu} + \eta_{inh})}$	0.2454	-0.7582
$\omega = \frac{\mu_P^2}{2\eta} = \frac{(I+A)^2}{4(I-A)}$	5.024	17.6790
E_T(Ha)	-856.0103	-856.3006
CPU time	5h06min55s	6h18min30s

According to previous studies [47,48], high E_{HOMO} value provides information about the electron donation ability of an inhibitor molecule to an empty metal orbital, while low E_{LUMO} value means that the molecule tends to accept electrons from metal orbitals. In this study, it results that BHPA has a high value of E_{HOMO} and a low value of E_{LUMO} therefore BHPA has a good potential to give and receive electrons from the metal. The analysis of Table 4 reveals that the protonated form has a good electron accepting property hence a strong adsorption on copper surface, which leads to a better inhibition efficiency of the studied molecule. These results confirm the high values of inhibition efficiencies obtained experimentally.

The molecule reactivity molecule can be related to its energy gap value which is the difference in energy between HOMO and LUMO ($\Delta E = E_{LUMO} - E_{HOMO}$) [49]. Indeed, when the energy gap decreases, the molecule reactivity increases, which leads to an increase in the inhibition efficiency, whereas the increase in energy gap favors the fall molecular reactivity. The analysis of energy gap value obtained indicates that the tested compound is reactive. The protonated form has a lower value than the neutral molecule

which suggests that BHPA becomes more reactive in its protonated form hence its better ability to bind to copper surface compared to neutral molecule. Figure 9 shows the distribution of the electron density of HOMO and LUMO orbitals of protonated and neutral forms of BHPA. It results that for the both forms, this distribution touches almost the whole molecule , revealing electronic conjugation of aromatic ring, double and triple bonds. These observations justify the good reactive character of BHPA.

According to some reports [50,51], there is no significant relationship between dipole moment (μ) and inhibition efficiency. This lack of consensus on the correlation between dipole moment and inhibition efficiency in the literature makes the interpretation of this parameter with experimental data complex. Analysis of dipole moment value obtained indicates a considerable difference between that of neutral molecule and that of protonated form. Based on these observations no link can be established.

The reactivity of a molecule is also related to its global softness (σ) and its global hardness (η) [52]. In fact the hardness of a compound is the level of resistance to deformation or polarization of substances under the effect of a chemical reaction. While hardness inverse called global softness (σ) [52], measures the ability of a chemical species to receive electrons. softness and hardness values in both forms clearly indicate the molecule is highly reactive in the protonated form. Thus, to receive electrons from the metal, the molecule tends to protonate. It is very obvious that BHPA good inhibition capacity obtained experimentally is due to its low resistance to deformation and its ability to receive electrons from copper.

For the calculation of fraction of transferred electrons (ΔN) according to Pearson electronegativity relation [53] we apply theoretical values: $\chi_{cu} = 4{,}98\ eV$ [54] and $\eta_{cu} = 0$ [55]. The results gathered in Table 4 show that electronegativity (χ) value of neutral molecule is lower than that of copper (4.98 eV) and ΔN>0, while electronegativity (χ) of protonated form is higher than that of copper with ΔN<0. These observations reveal that the compound donates electrons to copper in the neutral form and receives electrons from copper in its protonated form [56]. It is apparent from this study that protonation of an organic compound during corrosion inhibition of a metal enhances its reactivity and in this case its anticorrosive properties.

	BHPA neutral	BHPA Protonated
Optimized molecular structures	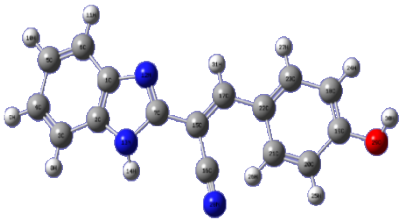	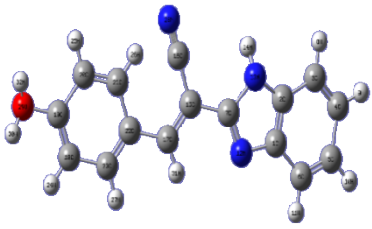
HOMO Orbitals	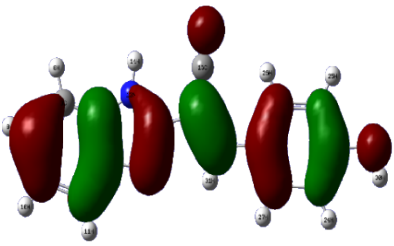	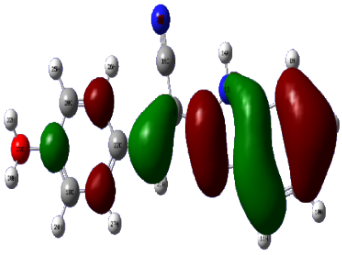
LUMO Orbitals	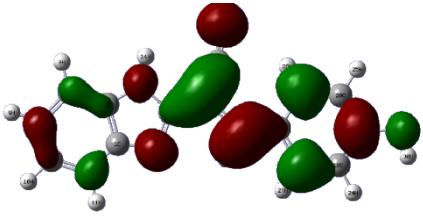	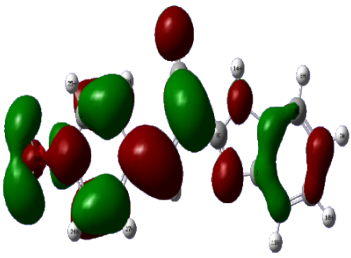

Figure 9. Electron density distribution of HOMO and LUMO orbitals for BHPA protonated and neutral forms.

Electrophilicity index (ω) was introduced by Yang and Parr [57] and its expression is electron affinity (A) and ionization energy (I) dependent. Electron affinity (A) measures the ability of a compound to accept a single electron while ionization energy measures the energy required to remove an electron. Electrophilicity index measures the ability of a compound to accept electrons [57]. The high ω value of BHPA obtained reveals that it is a good electrophile. This electrophilic character is more intense in the protonated form, so it appears that the protonated form accepts electrons from the metal more easily. This reactivity confirms the good inhibiting power observed experimentally.

Table 4 examination indicates that total energy (E_T) value of the protonated species is lower than neutral form, suggesting that protonated species is more reactive than neutral species [26]. Therefore, protonated species is more likely to adsorb onto the copper surface [58,59]. These results are in agreement with the experimental trends reported.

3.4.2. Reactivity active sites

In metal corrosion inhibition case by electron transfer, Fukui functions and dual descriptor give information on a molecule sites on which the nucleophilic, electrophilic or radical attacks are directed [60]. The active sites of reactivity identified by means of Fukui functions and dual descriptor permit to distinguish the chemical attitude of each atom within BHPA.

The condensed Fukui functions are computed calculated using the finite difference approximation where the electron density is replaced by an electron population q_k as given by the following expressions:

Nucleophilic attack $$f_k^+ = q_k(N+1) - q_k(N) \quad (13)$$

Electrophilic attack $$f_k^- = q_k(N) - q_k(N-1) \quad (14)$$

Radical attack $$f_k^0 = q_k(N+1) - q_k(N-1) \quad (15)$$

where $q_k(N+1)$, $q_k(N)$ and $q_k(N-1)$ are the atoms charges on the systems with $(N+1)$, N and $(N-1)$ electrons respectively.

Dual descriptor [61,62] can be calculated using the following equation:

$$\Delta f_k(r) = f_k^+ - f_k^- \quad (16)$$

Local descriptors values calculated using DFT/6-311G(d,p) are listed in Table 5.

According to the literature, the atoms with the highest values of f_k^+ and $\Delta f_k(r)$) represent the most probable sites for nucleophilic attacks while the atoms with the highest value of f_k^- and the lowest value $\Delta f_k(r)$) is the most probable center for electrophilic attacks.

Table 5 analysis clearly shows that O(29) atom is the most probable site for nucleophilic attacks while C(7) is the most probable site for electrophilic attacks.

Table 5. Calculated Mulliken atomic charges, Fukui functions and dual descriptor for BHPA.

Atom	$q_k(N+1)$	$q_k(N)$	$q_k(N-1)$	f_k^+	f_k^-	$\Delta f_k(r)$
1 C	0.071219	0.219662	-0.018246	-0.148443	0.237908	-0.386351
2 C	0.137517	0.219913	-0.005886	-0.082396	0.225799	-0.308195
3 C	-0.079898	-0.153486	0.018931	0.073588	-0.172417	0.246005
4 C	0.209819	-0.147031	0.029371	0.35685	-0.176402	0.533252
5 C	-0.016539	-0.150777	-0.008353	0.134238	-0.142424	0.276662
6 C	0.059359	-0.145776	0.043739	0.205135	-0.189515	0.39465
7 C	0.043808	0.433367	0.038086	-0.389559	**0.395281**	**-0.78484**
8 H	0.002652	0.143671	-0.001136	-0.141019	0.144807	-0.285826
9 H	-0.009379	0.142063	-0.001721	-0.151442	0.143784	-0.295226
9 H	0.000011	0.140400	0.000154	-0.140389	0.140246	-0.280635
10 H	-0.003245	0.150753	-0.002204	-0.153998	0.152957	-0.306955
12 N	0.108923	-0.542002	0.046281	0.650925	-0.588283	1.239208
13 N	-0.026299	-0.659538	0.029030	0.633239	-0.688568	1.321807
14 H	0.000395	0.341441	-0.001550	-0.341046	0.342991	-0.684037
15 C	0.155910	0.063392	0.047241	0.092518	0.016151	0.076367
16 C	-0.038962	0.319292	-0.009525	-0.358254	0.328817	-0.687071
17 C	0.014529	-0.169701	0.442348	0.18423	-0.612049	0.796279
18 C	0.006963	-0.206531	-0.100724	0.213494	-0.105807	0.319301
19 C	0.096436	0.347515	0.221179	-0.251079	0.126336	-0.377415
20 C	0.009911	-0.190067	-0.107361	0.199978	-0.082706	0.282684
21 C	0.018046	-0.148014	0.197730	0.16606	-0.345744	0.511804
22 C	0.092529	0.129413	-0.101347	-0.036884	0.23076	-0.267644
23 C	0.033330	-0.209526	0.172962	0.242856	-0.382488	0.625344
24 H	-0.000789	0.130704	0.003913	-0.131493	0.126791	-0.258284
25 H	-0.000856	0.154851	0.004179	-0.155707	0.150672	-0.306379
26 H	-0.001214	0.193707	-0.009610	-0.194921	0.203317	-0.398238
27 H	-0.001876	0.145171	-0.008657	-0.147047	0.153828	-0.300875
28 N	0.060269	-0.502297	0.074870	0.562566	-0.577167	1.139733
29 O	0.061109	-0.655466	0.029330	**0.716575**	-0.684796	**1.401371**
30 H	-0.002108	0.310799	-0.001339	-0.412907	0.412138	-0.625045
31 H	-0.001570	0.194097	-0.021683	-0.195667	0.21578	-0.411447

Figure 10 displays BHPA molecule with the natures and labels of the atoms allowing easier identification of the reactivity sites.

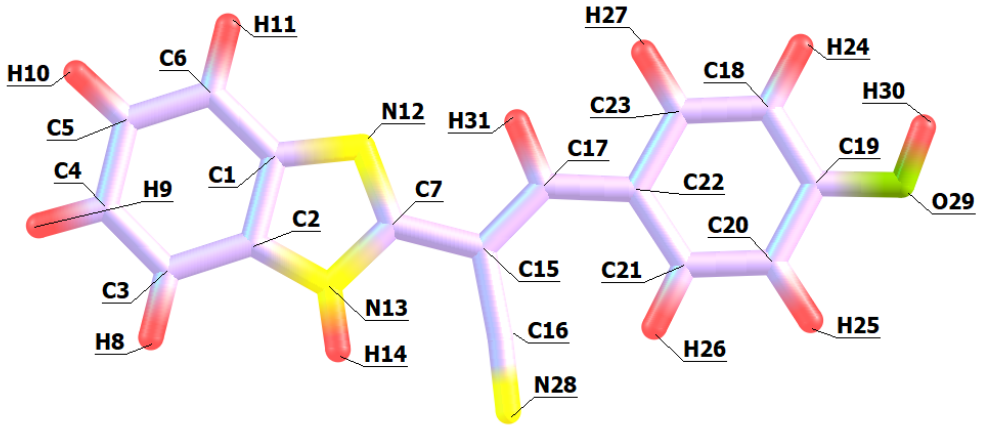

Figure 10. BHPA molecule with the natures and labels of the atoms.

3.4.3. Quantitative structure-property relationship (QSPR) consideration

This investigation by QSPR model was carried out on the basis of experimental data at 298K. Referring to the empirical linear model proposed by Lukovits *et al.* [34] equation (1) becomes:

$$IE_{calc}(\%) = \frac{[Ax_1 + Bx_2 + Dx_3 + E]C_i}{1 + [Ax_1 + Bx_2 + Dx_3 + E]C_i} * 100. \qquad (17)$$

Coefficients A, B, D and E values are determined based on the four concentrations ($1\mu M$, $6\mu M$, $10\mu M$ and $30\mu M$) of BHPA and a set of molecular quantum chemical parameters. Thus solving a system of four equations with four unknowns will yield these coefficients. These coefficients will allow to find equations or the best set of molecular quantum chemical parameters useful to predict the inhibition efficiency of molecules analogous to the studied compound. The calculations were investigated using the EXCEL software. Calculated inhibition efficiency versus experimental inhibition efficiencies is given by Figure 11a and 11b.

QSPR model validation is done from the statistical parameters whose expressions are given below:

The sum of square errors (SSE):

$$SSE = \sum_{i=1}^{N} \left(IE_{exp} - IE_{calc}\right)^2 \quad (18)$$

The root mean square error (RMSE):

$$RMSE = \sqrt{\frac{\sum_{i=1}^{N} \left(IE_{exp} - IE_{calc}\right)^2}{N}} \quad (18)$$

Tables 6 and 7 summarize different coefficients and statistical parameters values.

Table 6. Coefficients A, B, D and E, Coefficient determination (R^2) and SSE, RMSE values for BHPA neutral.

Set of parameters	A	B	D	E	R^2	SSE	$RMSE$
(σ,ω,I)	**41454.3716**	**1138.742**	**48310.9033**	**241004.291**	**0.9846**	**344.85**	**9.258**
(E_{LUMO},E_{HOMO},χ)	139.844324	2830.22891	-1852.85036	23381.7711	0.9819	418.92	10.234
$(\mu,\Delta E,\eta)$	-32.1846388	12.7930555	-42.7932846	110.733967	0.9696	699.07	26.440
$(A,\Delta N,E_{HOMO})$	$7.5049.10^{14}$	$-4.1309.10^{15}$	$-1.2555.10^{13}$	$-3.9199.10^{14}$	0.9794	484.26	11.003

Table 7. Coefficients A, B, D and E, Coefficient determination (R^2) and SSE, RMSE values for BHPA protonated.

Set of parameters	A	B	D	E	R^2	SSE	$RMSE$
(σ,ω,I)	**24686.6526**	**81.3092409**	**-41090.4071**	**339673.074**	**0.9838**	**368,05**	**9.593**
(E_{LUMO},E_{HOMO},χ)	20918.3157	1457.98327	1024.59882	124765.673	0.9656	837.77	14.472
$(\mu,\Delta E,\eta)$	3200.07071	-4555.78251	-3598.28268	-49349.8473	0.9612	14173,11	59.53
$(A,\Delta N,E_{HOMO})$	-9876.22138	4028.28126	$7.0037.10^{13}$	$6.1003.10^{14}$	0.9794	11276.88	53.094

As can be seen in Tables 6 and 7, it obviously appears that (σ,ω,I) with the lowest statistical parameters values for the neutral and protonated species with $R^2 > 0.98$ is the best set of molecular quantum chemical parameters for correlating experimental (IEexp (%)) and calculated inhibition efficiency (IEcalc(%)).The best set of molecular quantum chemical parameters which is global softness (σ), electrophilicity index(ω)and ionization energy (I) combination confirms the electron acceptor character of BHPA protonated form. This protonated form would be the inhibition process base. It is observed that the same set of molecular quantum chemical parameters allows to correlate BHPA inhibition efficiency and the molecular structures for the neutral and protonated species. Therefore, it is deduced that $BHPAH^+$ strongly participates in copper corrosion inhibition in nitric acid solution.

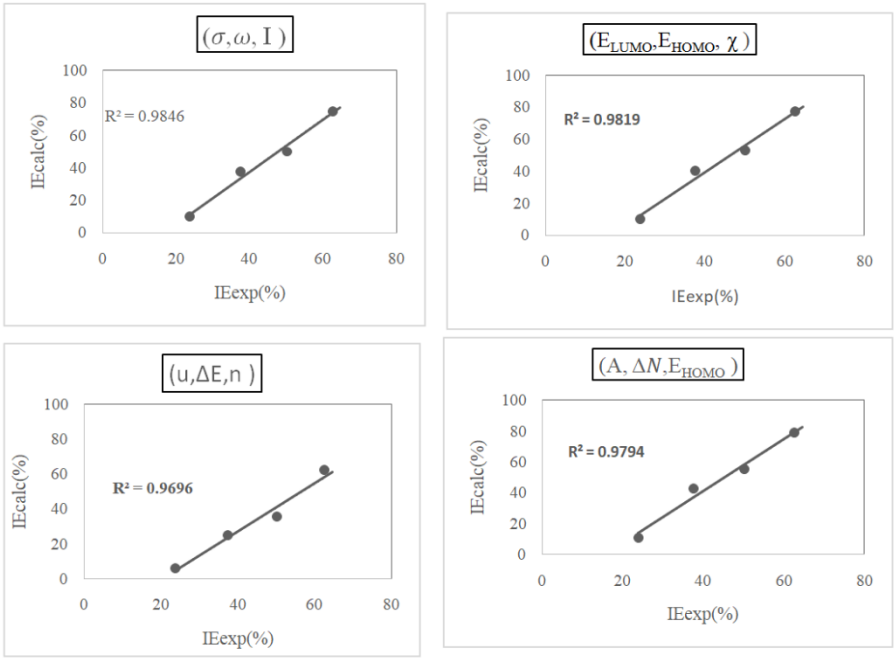

Figure 11a. IEcalc(%) versus IEexp(%) for BHPA neutral form.

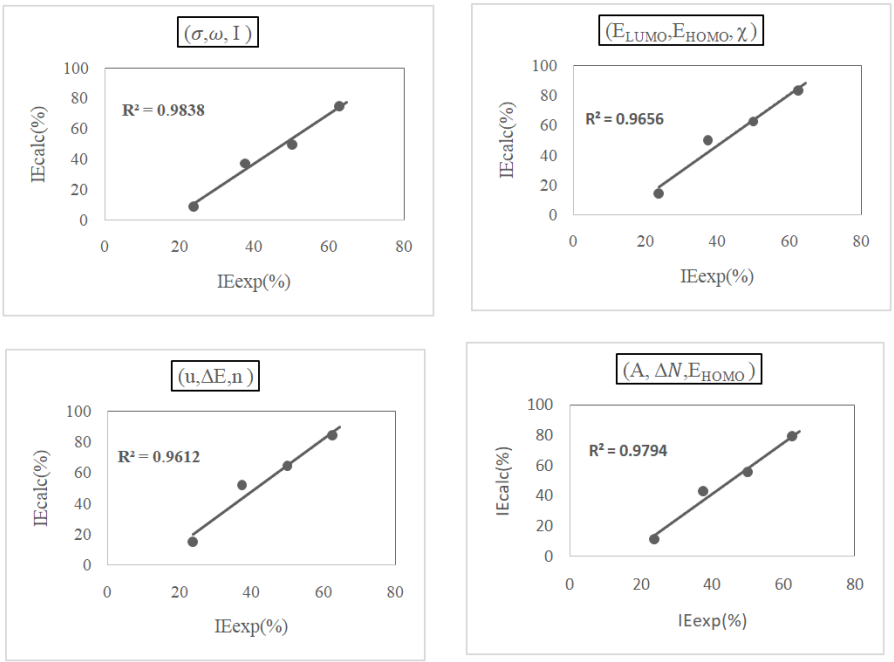

Figure 11b. IEcalc(%) versus IEexp(%) for BHPA protonated form.

3.5. Inhibition mechanism

The experimental data showed that BHPA adsorption on copper surface is dominated by chemisorption. Indeed BHPA is protonated in acid solution according to the following equation:

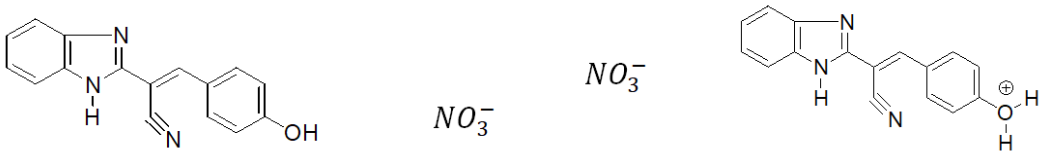

The comparison of quantum chemical parameters values of protonated species with those of neutral species indicates that the protonated form which has the lowest energy gap is more reactive. This reactivity occurs through electron acceptor donor between the incompletely filled d-orbitals of copper and the unshared electron pairs of the heteroatoms, which could explain the predominance of chemisorption. Moreover there are electrostatic interactions between NO_3^- ions on copper surface and the protonated species derived from the inhibitor which shows the existence of physisorption. This mechanism is described by the following schematic:

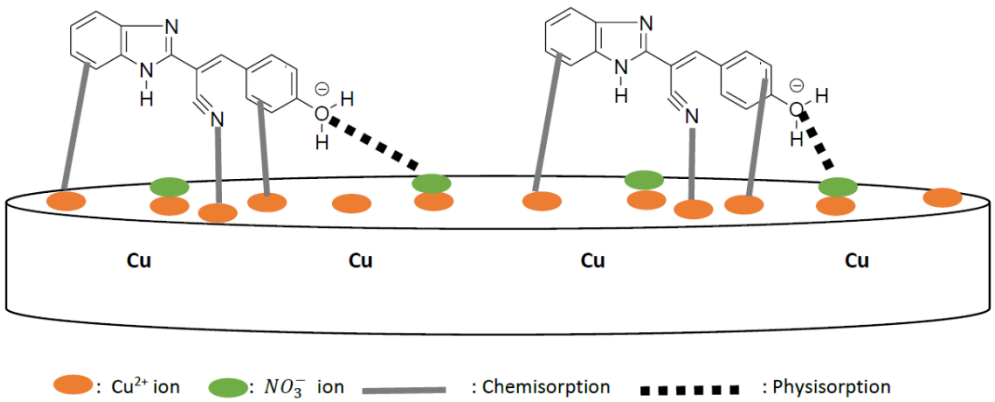

Figure 12. Pictorial representation of BHPAadsorption on copper surface in 1.0 M HNO_3.

4. Conclusion

This study focused on investigating the inhibition potential of 2-(1H-benzimidazol-2-yl)-3-(4-hydroxyphenyl) acrylonitrile in 1M HNO_3 by the experimental and theoretical

techniques. From the main results obtained, the following conclusions can be drawn:

- Gravimetric measurements clearly indicate that BHPA inhibition efficiency increases with temperature and concentration. So BHPA can protect copper against corrosion at high temperature with low concentrations.
- BHPA adsorption obeys the modified Langmuir model or Villamil model and Adejo-Ekwenchi isotherm reveals that this adsorption is dominated by chemisorption.
- Thermodynamic adsorption and activation parameters indicate a spontaneous, endothermic adsorption process, an increase in disorder and a Cu-Inh complex formation on copper surface, thus reducing copper dissolution in HNO_3.
- Quantum chemical calculations revealed that BHPA is highly reactive and in addition its protonated form facilitates inhibitor-copper interactions. These results allow us to conclude that protonated specie have more acceptor than electron donor properties.
- O(29) and C(7) are considered respectively as the nucleophilic and electrophilic attack centers.
- The insights gained from QSPR model permits to screen organic molecules of the same family before experimental validation. Therefore the set of parameters (σ,ω ,I) allows to perform this correlation.

Finally theoretical results are in agreement with the experimental data.

References

[1] Wang, W., Xu, R., Hao, Y., Wang, Q., Yu, L., Che, Q., *et al*. (2018). Corrosion fatigue behavior of friction stir processed interstitial free steel. *Journal Materials Science Technology*, *34*(1), 148-156. https://doi.org/10.1016/j.jmst.2017.11.013

[2] Tsai, H.Y., Sun, S.C., & Wang, S.J. (2000). Characterization of sputtered tantalum carbide barrier layer for copper metallization. *Journal of the Electrochemical Society*, *147*(7), 2766. https://doi.org/10.1149/1.1393604

[3] Ho, C.E., Chen, W.T., & Kao, C.R. (2001). Interactions between solder and metallization during long-term aging of advanced microelectronic packages. *Journal of Electronic Materials, 30*, 379-385. https://doi.org/10.1007/s11664-001-0047-6

[4] Simon, N.J., Drexler, E.S., & Reed, R.P. (1992). Properties of copper and copper alloys at cryogenic temperatures. Final report. *United States*. https://doi.org/10.2172/5340308

[5] Petrovic Mihajlovic, M.B., & Antonijevic, M.M. (2015). Copper corrosion inhibitors. Period 2008-2014. A review. *International Journal of Electrochemical Science*, *10*, 1027-1053.

[6] Sherif, E.M., & Park, S.-M. (2005). Inhibition of copper corrosion in 3.0% NaCl solution by *N*-phenyl-1,4-phenylenediamine. *Journal of the Electrochemical Society*, *152*(10), 428-433. https://doi.org/10.1149/1.2018254

[7] Finšgar, M. (2013). EQCM and XPS analysis of 1,2,4-triazole and 3-amino-1,2,4-triazole as copper corrosion inhibitors in chloride solution. *Corrosion Science*, *77*, 350-359. https://doi.org/10.1016/j.corsci.2013.08.026

[8] Otmacic, H., & Stupnisek-Lisac, E. (2003). Copper corrosion inhibitors in near neutral media. *Electrochimica Acta*, *48*(8), 985-991. https://doi.org/10.1016/S0013-4686(02)00811-3

[9] Gasparac, R., Martin, C.R., & Stupnisek-Lisac, E. (2000). *In situ* studies of imidazole and its derivatives as copper corrosion inhibitors. I. Activation energies and thermodynamics of adsorption. *Journal of the Electrochemical Society*, *147*(2), 548-551. https://doi.org/10.1149/1.1393230

[10] Parook Feroz, K., Vaithianathan, S., Rupesh, K.B., Srinivasan, M., & Rakesh, C.B. (2015). Effect of benzotriazole on corrosion inhibition of copper under flow conditions. *Journal of Environmental Chemical Engineering*, *3*(1), 10-19. https://doi.org/10.1016/j.jece.2014.11.005

[11] Hollander, O., & May, R.C. (1985). The chemistry of azole copper corrosion inhibitors in cooling waters. *Corrosion*, *41*, 39-45. https://doi.org/10.5006/1.3581967

[12] Singh, K., Kumar, Y., Puri, P., Kumar, M., & Sharma, C. (2012). Cobalt, nickel, copper and zinc complexes with 1,3-diphenyl-1H-pyrazole-4-carboxaldehyde Schiff bases: Antimicrobial, spectroscopic, thermal and fluorescence studies. *European Journal of Medicinal Chemistry*, *52*, 313-321. https://doi.org/10.1016/j.ejmech.2012.02.053

[13] Uhlig, H.H., & King, P.F. (1959). The Flade potential of iron passivated by various inorganic corrosion inhibitors. *Journal of the Electrochemical Society*, *106*, 1-7. https://doi.org/10.1149/1.2427255

[14] Aben, T., & Tromans, D. (1995). Anodic polarization behavior of copper in aqueous bromide and bromide/benzotriazole solutions. *Journal of the Electrochemical Society*, *142*, 398-404. https://doi.org/10.1149/1.2044031

[15] Falluvena, T., Antonow, M., & Goncalves, R.S. (2006). Caffeine as non-toxic corrosion inhibitor for copper in aqueous solutions of potassium nitrate. *Applied Surface Science*, *253*(2), 566-571. https://doi.org/10.1016/j.apsusc.2005.12.114

[16] Simonovic, A.T., Petrovic, M.B., Radonavovic, M.B., Milik, S.M., & Antonijevic, M.M. (2014). Inhibition of copper corrosion in acid sulphate media by eco-friendly amino acid compound. *Slovak Academy of Sciences*, *68*(3), 1-10. https://doi.org/10.2478/s11696-013-0458-x

[17] Scendo, M. (2008). Inhibition of copper corrosion in sodium nitrate solutions with nontoxic inhibitors. *Corrosion Science*, *50*, 1584-1592. https://doi.org/10.1016/j.corsci.2008.02.015

[18] Scendo, M. (2007c). Corrosion inhibition of copper by purine or adenine in sulphate solutions. *Corrosion Science*, *49*, 3953-3968. https://doi.org/10.1016/j.corsci.2007.03.037

[19] El-Naggar, M.M. (2000). Bis-triazole as a new corrosion inhibitor for copper in sulfate solution. A model for synergistic inhibition action. *Journal of Materials Science*, *35*, 6189-6195. https://doi.org/10.1023/A:1026725110344

[20] Gomma, G.K., & Wahdan, M.H. (1994). Effect of temperature on the acidic dissolution of copper in the presence of amino acids. *Materials Chemistry and Physics*, *39*, 142-148. https://doi.org/10.1016/0254-0584(94)90191-0

[21] El Issami, S., Bazzi, L., Mihit, M., Hammouti, B., Kerit, S., Addi, E.A., & Salghi, R. (2007). Triazolic compounds as corrosion inhibitors for copper in hydrochloric acid. *Pigment & Resin Technology*, *36*, 161-168. https://doi.org/10.1108/03699420710749027

[22] Khaled, K.F. (2008). Adsorption and inhibitive properties of a new synthesized guanidine derivative on corrosion of copper in 0.5 M H_2SO_4. *Applied Surface Science*, *255*, 1811-1818. https://doi.org/10.1016/j.apsusc.2008.06.030

[23] Fucks-Godec, R., & Zergav, G. (2015) Corrosion resistance of high-level hydrophobic layers combination with vitamin E-(α-tocopherol) as green inhibitor. *Corrosion Science*, *97*, 7-16. https://doi.org/10.1016/j.corsci.2015.03.016

[24] Gokhan, G. (2011). Drugs: A review of promising novel corrosion inhibitors. *Corrosion Science*, *53*, 3873-3898. https://doi.org/10.1016/j.corsci.2011.08.006

[25] Kouakou, V., Niamien, P.M., Yapo, A.J., Diaby, S., & Trokourey, A. (2016). Experimental and DFT studies on the behavior of caffeine as effective corrosion inhibitor of copper in 1M HNO_3. *Orbital. The Electronic Journal of Chemistry*, *8*(2), 66-79. https://doi.org/10.17807/orbital.v8i2.804

[26] El Faydy, M., Benhiba, F., About, H., Kerroum, Y., Guenbour, A., Lakhrissi, B., Warad, I., Verma, C., Sherif, El-Sayed M., Ebenso, E. E., & Zarrouk, A. (2020). Experimental and

computational investigations on the anti-corrosive and adsorption behavior of 7N,N'-dialkyaminomethyl-8-Hydroxyquinolines on C40E steel surface in acidic medium. *Journal of Colloid and Interface Science*, *576*, 330-344. https://doi.org/10.1016/j.jcis.2020.05.010

[27] Khalifa, M.E., El Azab, I.H., Gobouri, A.A., Mersal, G.A.M., Alharthi, S., Saracoglu, M., Kandemirli, F., Ryl, J., & Amin, M.A. (2020). Adsorption behavior and corrosion inhibitive characteristics of newly synthesized cyano-benzylidene xanthenes on copper/sodium hydroxide interface: Electrochemical, X-ray photoelectron spectroscopy and theoretical studies. *Journal of Colloid and Interface Science*, *580*, 108-125. https://doi.org/10.1016/j.jcis.2020.06.110

[28] Niamien, P.M., Essy, F.K., Trokourey, A., Yapi, A., Aka, H.K., & Diabate, D. (2012). Correlation between the molecular structure and the inhibiting effect of some benzimidazole derivatives. *Materials Chemistry and Physics*, *136*, 59-65. https://doi.org/10.1016/j.matchemphys.2012.06.025

[29] Tigori, M.A., Kouyaté, A., Kouakou, V., Niamien, P.M., & Trokourey, A. (2020). Computational approach for predicting the adsorption properties and inhibition of some antiretroviral drugs on copper corrosion in HNO_3. *European Journal of Chemistry*, *11*(3), 235-244. https://doi.org/10.5155/eurjchem.11.3.235-244.2011

[30] Tigori, M.A., Kouyaté, A., Kouakou, V., Niamien, P.M., & Trokourey A. (2020). Inhibition performance of some sulfonylurea on copper corrosion in nitric acid solution evaluated theoretically by DFT calculations. *Open Journal of Physical Chemistry*, *10*(3), 139-157. https://doi.org/10.4236/ojpc.2020.103008

[31] Van Allan, J.A., & Deagon, B. D. (1963). *Organic syntheses collect* (vol. 4). John Wiley & Sons, New York, NY, USA.

[32] Frisch, M.J., Trucks, G.W., Schlegel, H.B., Scuseria, G.E., Robb, M.A., Cheeseman, J.R., Scalmani, G., Barone, V., Mennucci, B., Petersson, G.A., Nakatsuji, H., Caricato, M., Li, X., Hratchian, H.P., Izmaylov, A.F., Bloino, J., Zheng, G., Sonnenberg, J.L., Hada, M., Ehara, M., Toyota, K., Fukuda, R., Hasegawa, J., Ishida, M., Nakajima, T., Honda, Y., Kitao, O., Nakai, H., Vreven, T., Montgomery, Jr., Peralta, J.E., Ogliaro, F., Bearpark, M., Heyd, J.J., Brothers, E., Kudin, K.N., Staroverov, V.N., Kobayashi, R., Normand, J., Raghavachari, K., Rendell, A., Burant, J.C., Iyengar, S.S., Tomasi, J., Cossi, M., Rega, N., Millam, J.M., Klene, M., Knox, J.E., Cross, J.B., Bakken, V., Adamo, C., Jaramillo, J., Gomperts, R., Stratmann, R.E., Yazyev, O., Austin, A.J., Cammi, R., Pomelli, C., Ochterski, J.W., Martin, R.L., Morokuma, K., Zakrzewski, V.G., Voth, P., Salvador, G.A., Dannenberg, S., Dapprich, J.J., Daniels, A.D., Farkas, Ö., Foresman, J.B., Ortiz, J.V., Cioslowski, J., & Fox, A.D. (2009). *J. Gaussian 09. Gaussian, Inc*., Wallingford, CT.

[33] Becke, A.D. (1992). Density-functional thermochemistry. I. The effect of the exchange-only gradient correction. *The Journal of Chemical Physics*, *96*, 2155-2160. https://doi.org/10.1063/1.462066

[34] Lukovits, I., Shaban, A., & Kalman, E. (2003). Corrosion inhibitors: Quantitative structure–activity relationships. *Russian Journal of Electrochemistry*, *39*, 177-181. https://doi.org/10.1023/A:1022313126231

[35] Khaled, K.F. (2006). Experimental and theoretical study for corrosion inhibition of mild steel in hydrochloric acid solution by some new hydrazine carbodithioic acid derivatives. *Applied Surface Science*, *252*(12), 4120-4128. https://doi.org/10.1016/j.apsusc.2005.06.016

[36] Langmuir, I. (1916). The constitution and fundamental properties of solids and liquids. *Journal of the American Chemical Society*, *38*(11), 2221-2295. https://doi.org/10.1021/ja02268a002

[37] Villamil, R.F.V., Corio P., Rubin, J.C., & Agostinho, S.M.L. (1999). Effect of sodium dodecyl sulfate on copper corrosion in sulfuric acid media in the absence and presence of benzotriazole. *Journal of Electro Analytical Chemistry*, *472*, 112-116. https://doi.org/10.1016/S0022-0728(99)00267-3

[38] Zhou, L., Zhang, S., Tan, B., Feng, L., Xiang, B., Chen, F., Li, W., Xiong, B., & Song, T. (2020). Phenothiazine drugs as novel and eco-friendly corrosion inhibitors for copper in sulfuric acid solution. *Journal of the Taiwan Institute of Chemical Engineers*, *113*, 253-263. https://doi.org/10.1016/j.jtice.2020.08.018

[39] Ye, Y., Yang, D., Chen, H., Guo, S., Yang, Q., Chen, L., Zhao, H., & Wang, L. (2020). A high-efficiency corrosion inhibitor of N-doped citric acid-based carbon dots for mild steel in hydrochloric acid environment. *Journal of Hazardous Materials*, *381*, 121019. https://doi.org/10.1016/j.jhazmat.2019.121019

[40] Oubaaqa, M., Rbaa, M., Ouakki, M. *et al.* (2022). Novel triphenyl imidazole based on 8-hydroxyquinoline as corrosion inhibitor for mild steel in molar hydrochloric acid: experimental and theoretical investigations. *Journal of Applied Electrochemistry*, 52, 413-433. https://doi.org/10.1007/s10800-021-01632-3

[41] Yadav, M., Behera, D., & Sharma, U. (2016). Nontoxic corrosion inhibitors for N80 steel in hydrochloric acid. *Arabian Journal of Chemistry*, 9, S1487-S1495. https://doi.org/10.1016/j.arabjc.2012.03.011

[42] Ramesh Saliyan, V., & Adhikari, A.V. (2008). Inhibition of corrosion of mild steel in acid media by N′-benzylidene-3-(quinolin-4-ylthio)propanohydrazide. *Bull. Mater. Sci.*, *31*, 699-711. https://doi.org/10.1007/s12034-008-0111-4

[43] Adejo, S.O., Ahile, J.U., Gbertyo, J.A., Kaior, A., & Ekwenchi, M.M. (2014). Resolution of adsorption characterisation ambiguity through the Adejo-Ekwenchi adsorption isotherm: a case study of leaf extract of Hyptis suaveolen poit as green corrosion inhibitor of corrosion of mild steel in 2 M HCl. *Journal of Emerging Trends in Engineering and Applied Sciences*, 5 , 201-205. https://doi.org/10.10520/EJC157010

[44] Parul, D., Ansaria, K.R., Quraishia, M.A., & Obot, I.B. (2017). Pyranpyrazole derivatives as novel corrosion inhibitors for mild steel useful for industrial pickling process: experimental and quantum chemical study. *Journal of Industrial and Engineering Chemistry*, *52*, 197-210. https://doi.org/10.1016/j.jiec.2017.03.044

[45] Motawea, M.M., El-Hossiany, A., & Fouda, A.S. (2019). Corrosion control of copper in nitric acid solution using Chenopodium extract. *International Journal of Electrochemical Science*, *14*, 1372-1387. https://doi.org/10.20964/2019.02.29

[46] Khattabi, M., Benhiba, F., Tabti, S., Djedouani, A., El Assyry, A., Touzani, R., Warad, I., Oudda, H., & Zarrouk, A. (2019). Performance and computational studies of two soluble pyran derivatives as corrosion inhibitors for mild steel in HCl. *Journal of Molecular Structure*, *1196*, 231-244. https://doi.org/10.1016/j.molstruc.2019.06.070

[47] Qiang, Y., Zhang, S., Guo, L., Zheng, X., Xiang, B., & Chen, S. (2017). Experimental and theoretical studies of four allyl imidazolium-based ionic liquids as green inhibitors for copper corrosion in sulfuric acid. *Corrosion Science*, *119*, 68-78. https://doi.org/10.1016/j.corsci.2017.02.021

[48] Kumar, D., Jain, N., Jain, V., & Rai, B. (2020). Amino acids as copper corrosion inhibitors: A density functional theory approach. *Applied Surface Science*, *514*, 145905. https://doi.org/10.1016/j.apsusc.2020.145905

[49] Saira, F., Renu, S., Faiza, A., Ajar, K., Amin, B., & Heinz-Bernhard, K. (2019). Study of new amphiphiles based on ferrocene containing thioureas as efficient corrosion inhibitors: Gravimetric, electrochemical, SEM and DFT studies. *Journal of Industrial and Engineering Chemistry*, *76*, 374-387. https://doi.org/10.1016/j.jiec.2019.04.003

[50] Rodriguez-Valdez, L.M., Martinez-Villafane, A., & Glossman Mitnik, D. (2005). Computational simulation of the molecular structure and properties of heterocyclic organic compounds with possible corrosion inhibition properties. *Journal of Molecular Structure: THEOCHEM*, *713*(1-3), 65-70. https://doi.org/10.1016/j.theochem.2004.10.036

[51] El Hassani, A.A., El Adnani, Z., Benjelloun, A.T., *et al*. (2020). DFT theoretical study of 5-(4-R-phenyl)-1*H*-tetrazole (R = H; OCH_3; CH_3; Cl) as corrosion inhibitors for mild steel in hydrochloric acid. *Metals and Materials International*, *26*, 1725-1733. https://doi.org/10.1007/s12540-019-00381-5

[52] Yang, W., & Parr, R.G. (1985). Hardness, softness and the Fukui function in the electronic theory of metals and catalysis. *Proceedings of the National Academy of Science*, 82(20), 6723-6726. https://doi.org/10.1073/pnas.82.20.6723

[53] Pearson, R.G. (1990). Hard and soft acids and bases-the evolution of a chemical concept. *Coordination Chemistry Reviews*, *100*(C), 403-425. https://doi.org/10.1016/0010-8545(90)85016-L

[54] Michaelson, H.B. (1977). The work function of the elements and its periodicity. *Journal of Applied Physics*, *48*, 4729-4733. https://doi.org/10.1063/1.323539

[55] Dewar, M.J.S., Zoebisch, E.G., Healy, E.F., & Stewart, J.P. (1985). Development and use of quantum mechanical molecular models. 76. AM1: a new general purpose quantum mechanical molecular model. *Journal of the American Chemical Society*, *107*(13), 3902-3909. https://doi.org/10.1021/ja00299a024

[56] Lukovits, I., Kálmán, E., & Zucchi, F. (2001). Corrosion inhibitors—correlation between electronic structure and efficiency. *Corrosion*, *57*(1), 3-8. https://doi.org/10.5006/1.3290328

[57] Parr, R.G., Sventpaly, L., & Liu, S. (1999). Electrophilicity index. *Journal of the American Chemical Society*, *121*(9), 1922-1924. https://doi.org/10.1021/ja983494x

[58] Zarrouk, A., Hammouti, B., Dafali, A., Bouachrine, M., Zarrok, H., Boukhris, S., & Al-Deyab, S.S. (2014). A theoretical study on the inhibition efficiencies of some quinoxalines as corrosion inhibitors of copper in nitric acid. *Journal of Saudi Chemical Society*, *18*, 450-455. https://doi.org/10.1016/j.jscs.2011.09.011

[59] Ansari, K.R., Quraishi, M.A., & Ambrish S. (2015). Pyridine derivatives as corrosion inhibitors for N80 steel in 15%HCl: Electrochemical, surface and quantum chemical studies. *Measurement*, *76*, 136-147. https://doi.org/10.1016/j.measurement.2015.08.028

[60] Parr, R.G., & Yang, W. (1984). Density functional approach to the frontier-electron theory of chemical reactivity. *Journal of the American Chemical Society*, *106*(14), 4049-4050. https://doi.org/10.1021/ja00326a036

[61] Morell, C., Grand, A., & Toro-Labbé, A. (2005). New dual descriptor for chemical reactivity. *Journal of Physical Chemistry A*, *109*(1), 205-212. https://doi.org/10.1021/jp046577a

[62] Martínez-Araya, J.I. (2015). Why is the dual descriptor a more accurate local reactivity descriptor than Fukui functions?. *Journal of Mathematical Chemistry*, *5*, 451-465. https://doi.org/10.1007/s10910-014-0437-7